Precipitable Water Vapour Estimation from GNSS Observations: Methodology and Evaluation during a High-Precipitation Month in Santa Maria (RS)

Afonso M. Albuquerque[1], Tayná A. F. Gouveia[1], Daniele B. M. Alves[1]

Faculty of Science and Technology, São Paulo State University, Presidente Prudente, Brazil[1]

Keywords: Precipitable Water Vapour (PWV); Rainfall; Global Navigation Satellite Systems (GNSS); Zenith Wet Day (ZWD).

Abstract

Precipitable Water Vapour (PWV) represents the total amount of water vapour contained in a vertical column of the atmosphere that is available for precipitation. It is a key variable in meteorological studies, as well as in the monitoring of extreme weather events. This study proposes and evaluates a method for estimating PWV using Global Navigation Satellite System (GNSS) data (PWV-GNSS), obtained from the Zenith Total Delay (ZTD), which comprises the Zenith Hydrostatic Delay (ZHD) and the Zenith Wet Delay (ZWD). The approach combines data from GNSS stations with external meteorological sources to improve atmospheric monitoring systems. The evaluation was conducted in the region of Santa Maria, Brazil (RS), selected due to the proximity (~2km) between the radiosonde (SBSM), GNSS (SMAR), and meteorological (A803) stations and its variable climate, characterised by frequent precipitation events. As a case study, the month of September 2023 was analysed, during which accumulated rainfall exceeded 450 mm. Results indicated strong agreement between PWV estimates derived from GNSS (PWV-GNSS) and radiosonde observations (PWV-RDS) used as a reference, with a root mean square error (RMSE) of 2.37 mm, a bias of –1.90 mm, and a coefficient of determination (R^2) of 0.97 between PWV-RDS and PWV-GNSS. Furthermore, PWV-GNSS demonstrated a characteristic response to heavy rainfall events, with reductions of up to 40 mm following intense precipitation.

1. Introduction

The neutrosphere is a layer of the atmosphere that extends from the Earth's surface to approximately 50 km in altitude, encompassing both the troposphere and stratosphere regions, which are studied in meteorology. Introduced by Chapman (1950), the term neutrosphere refers to the portion of the atmosphere not significantly affected by ionisation (Elgered and Wickert, 2017). The neutrosphere causes significant errors in GNSS (Global Navigation Satellite Systems) positioning, ranking second only to the ionosphere. The neutrospheric delay is caused by the atmospheric composition, which includes dry gases such as oxygen and hydrogen (hydrostatic component), as well as water vapour (non-hydrostatic component) (Saastamoinen, 1973; Davis et al., 1985; Vianello & Alves, 2000; Sapucci, 2001; Elgered & Wickert, 2017; Gouveia et al., 2020).

Variations in the refractive index of neutrosphere constituents lead to the Zenith Total Delay (ZTD), affecting the propagation of electromagnetic waves in both direction and speed (Thayer, 1974; Hofmann-Wellenhof et al., 2007). Under typical atmospheric conditions, the ZTD can exceed 2.3 metres for satellites near the zenith and may increase by an order of magnitude for those near the horizon (Seeber, 2003; Monico, 2008; Teunissen and Montenbruck, 2017). The ZTD has two parts: the Zenith Hydrostatic Delay (ZHD), which accounts for about 90% of the total delay and mainly originates from dry atmospheric gases, and the Zenith Wet Delay (ZWD), which varies significantly depending on the amount of water vapour in the atmosphere (Bevis et al., 1992; Sapucci, 2001; Nievinski and Santos, 2010; Gouveia et al., 2020).

Atmospheric water vapour, which is most concentrated within the first few kilometres above the Earth's surface and extends up to approximately 10 km in altitude, directly influences the Zenith Wet Delay (ZWD) (Bevis et al., 1992; Vianello and Alves, 2012; Elgered and Wickert, 2017; Gouveia et al., 2020). Its magnitude varies according to the climatic and geographical characteristics of each region (Sapucci, 2001; Wallace and Hobbs, 2006; Vianello and Alves, 2012). Humid environments, such as the Amazon rainforest, tropical biomes, and areas with frequent or intense rainfall, typically exhibit higher atmospheric moisture content (Vianello and Alves, 2012; Gouveia et al., 2020), which contributes to increased ZWD values. These variations, influenced by seasonal changes and extreme weather events, make the ZWD a particularly challenging parameter to model and predict accurately (Elgered and Wickert, 2017).

One of the most accurate instruments for determining the ZWD is the radiosonde (RDS) (Sapucci, 2001; Gouveia et al., 2020), also known as Upper-Air Stations (UAS), which can collect meteorological parameters at various altitude levels (Albuquerque et al., 2024). In this context, meteorological parameters allow integrating the ZWD as a function of altitude (Sapucci, 2001; Gouveia et al., 2020). This methodology makes UAS a reference for ZWD estimation and validation analyses.

While the neutrosphere introduces positioning errors in GNSS systems through ZTD, it serves as a valuable source of information, as in meteorology. ZWD can be converted into Integrated Water Vapour (IWV), a metric that quantifies the total amount of water vapour within a vertical atmospheric column (Sapucci, 2005). The IWV can then be transformed into Precipitable Water Vapour (PWV), which expresses the amount of water vapour that could potentially condense and precipitate, measured in millimetres (Sapucci, 2005; Gouveia et al., 2020).

PWV is a key atmospheric variable for monitoring atmospheric humidity and has demonstrated significant potential in short-term rainfall prediction. Recent studies, such as Liu et al. (2022), indicate that integrating GNSS-derived PWV measurements with machine learning approaches can enhance both the accuracy and timeliness of weather forecasts, thereby enabling more reliable prediction of rainfall events (Sapucci, 2019; Liu et al., 2022; Xu et al., 2025). PWV is an important data source for operational meteorology, used in Numerical Weather Prediction (NWP) models (Rohm et al., 2014; Lu et al., 2017; Gong et al., 2023). It can also be assimilated into machine learning–based models,

This contribution has been peer-reviewed. The double-blind peer-review was conducted on the basis of the full paper.
https://doi.org/10.5194/isprs-annals-X-3-W4-2025-9-2026 | © Author(s) 2026. CC BY 4.0 License.

which have demonstrated promising results in various meteorological applications (Li et al., 2024; Albuquerque et al., 2024).

Although UAS provides accurate measurements of PWV, their temporal resolution is limited by the frequency of meteorological balloon launches, which typically occur every 8 to 12 hours. Additionally, the cost per launch can exceed 200 USD and is subject to risks such as equipment loss (Valencia, 2019).

Although high-precision GNSS equipment can be expensive, it enables the acquisition of continuous ZTD-GNSS data, from which PWV can be estimated 24 hours a day, with temporal resolutions ranging from 1–2 hours to even minutes. Simplified models calculate the ZHD, and subtracting it from the ZTD derives the ZWD. However, the most accurate approach involves using data from a meteorological station co-located with the GNSS receiver. In Brazil, there are currently around 147 operational GNSS stations, but many do not actively provide meteorological data (RBMC, 2025). As an alternative, researchers can use external meteorological datasets, such as those provided by the National Institute of Meteorology (INMET). INMET operates over 500 automatic surface weather stations across Brazil with hourly data resolution (INMET, 2025).

In this context, GNSS can provide a higher temporal resolution in PWV estimation compared to UAS, along with significantly lower operational value. Through GNSS data processing, ZTD can be estimated, for example, on an hourly basis, as provided by the SIRGAS (Geocentric Reference System for South America) for stations throughout South America (SIRGAS, 2025). Moreover, while there are approximately 43 UAS across Brazil (UW, 2025), the number of GNSS stations is at least three times higher. When combined with nearby INMET weather stations, these GNSS stations represent a practical and cost-effective alternative for obtaining PWV-GNSS.

This study uses ZTD-SIRGAS data to derive the ZWD by subtracting the ZHD, which is estimated from surface meteorological parameters obtained from automatic stations and applied to empirical models, such as those proposed by Saastamoinen (1972) and refined by Davis (1985). This approach enables the subsequent calculation of PWV.

The current research aims to evaluate the accuracy and applicability of PWV-GNSS as a tool for atmospheric monitoring and precipitation analysis in Brazil. By comparing PWV-GNSS with PWV-RDS and focusing on periods of intense rainfall in Santa Maria (RS), the research demonstrates the potential of GNSS systems to enhance the continuous monitoring of atmospheric water vapour. The approach provides an efficient method for PWV estimation, contributing to meteorology and climatology, especially in countries with limited observational infrastructure. Ultimately, this work highlights the role of GNSS technology in improving the detection and understanding of extreme precipitation events through higher temporal resolution and broader spatial coverage. This study focuses on the practical evaluation of GNSS-derived PWV as a tool for atmospheric monitoring and rainfall analysis, addressing the needs of applied meteorology in Brazil.

2. Data and methods

2.1 Dataset

The ZTD-GNSS is provided by the SIRGAS network (ZTD-SIRGAS) as daily files with hourly sampling, available via FTP (File Transfer Protocol). The SIRGAS network delivers high-precision ZTD estimates, with a mean Root Mean Square (RMS) error of approximately 7.5 mm and a mean bias of about -2 mm in relation to ZTD obtained from radiosonde observations (SIRGAS, 2025).

The meteorological stations from INMET have sensors that measure atmospheric pressure, temperature, relative humidity, and accumulated precipitation (INMET, 2025). We combined the ZTD-SIRGAS data from the GNSS station (SMAR) with meteorological parameters collected hourly by the INMET automatic station (A803) to obtain hourly PWV-GNSS estimates.

The Santa Maria (RS) region was selected for this study due to the presence of GNSS, INMET, and RDS stations within a 2 km radius, as well as its history of extreme precipitation events. Figure 1 presents the map of the stations in Santa Maria (RS).

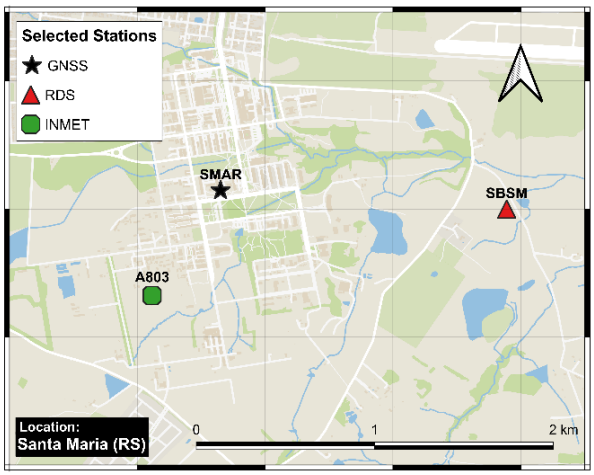

Figure. 1. Location map of stations in Santa Maria (RS), including Radiosonde (RDS), GNSS, and INMET meteorological stations.

The distance between the stations is a crucial factor in the analysis of precipitation events using PWV, as it ensures that the measurements represent the same atmospheric conditions. Proximal stations allow for the assessment of PWV levels at the precise time of rainfall (Barry and Blanken, 2016). In this study, the selected RDS, GNSS, and INMET stations are located within 1.6 km of each other. Table 1 lists the stations used, along with their geometric distances in kilometres relative to the GNSS station.

Station Type	Station ID	Elevation (m)	Distance from GNSS station (km)
RDS	SBSM	85.0	1.60
GNSS	SMAR	113.1	
INMET	A803	103.1	0.78

Table 1. Stations in Santa Maria (RS) and Distances from the GNSS Station to RDS and INMET Stations (in kilometres).

The distance between RDS and GNSS stations is approximately 1.6 km, while the GNSS station is located about 780 metres from the INMET station. Thus, precipitation events occur within the

This contribution has been peer-reviewed. The double-blind peer-review was conducted on the basis of the full paper.
https://doi.org/10.5194/isprs-annals-X-3-W4-2025-9-2026 | © Author(s) 2026. CC BY 4.0 License.

effective range of all stations involved in this study, enabling a robust analysis. The UAS in the Santa Maria region (RS) collected data twice daily, at 00:00 and 12:00 UTC (Coordinated Universal Time), whereas the GNSS and INMET stations operated continuously, providing data with hourly sampling over a 24-hour period.

2.2 Analysis of time series of extreme rainfall events

To define the study period, an analysis was conducted to identify the months with the highest accumulated precipitation in the region of Santa Maria (RS), based on data from the INMET automatic weather station (A803).

The precipitation events analysed for this region cover the period up to 2023, for which a complete dataset is available. Figure 2 shows the accumulated precipitation from 2014 to 2023 in Santa Maria (RS).

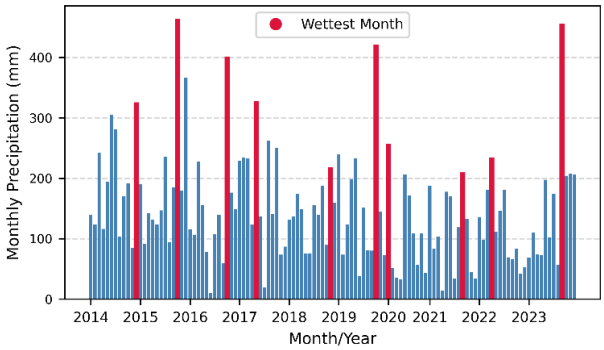

Figure 2. Time Series of Monthly Accumulated Precipitation from 2014 to 2023 at Station A803 in Santa Maria (RS).

Over the time series, four months recorded accumulated precipitation exceeding 400 mm. The most recent, September 2023, experienced 144 precipitation events and totalled 454 mm of rainfall. We selected September 2023 as the case study period because it is recent and has data available from all sources: GNSS, INMET, and RDS.

2.3 PWV from Radiosonde

The Neutrosphere Research Group at FCT-UNESP developed NEPTool (Neutrospheric Evaluation and Processing Tool) (Lima et al., 2022; Albuquerque et al., 2022; Albuquerque et al., 2024) to calculate zenith delay and PWV using data from RDS profiles. We used this software to generate PWV-RDS data for 2023 at the SBSM station.

NEPTool, coded in MATLAB, reads atmospheric profiles and integrates meteorological parameters across altitude levels (Bevis et al., 1992; Sapucci, 2001; Gouveia et al., 2020). Thus, the Equation (1) expresses the ZWD as:

$$ZWD = 10^{-6} \int_{h_s}^{h_{top}} \left(k_2' \frac{e}{T} Z_w^{-1} + k_3 \frac{e}{T^2} Z_w^{-1} \right) dh. \quad (1)$$

In this expression, temperature (T) uses Kelvin, while the partial pressure of water vapour (e) uses hPa. Z_w^{-1} denotes the inverse compressibility constant of non-hydrostatic gases. The atmospheric refractivity coefficients k_2' and k_3 used was determined by Rüeger (2002).

Using the Mean Temperature (Tm) and ZWD, it is possible to obtain IWV as follows in Equation (2) (Sapucci, 2001):

$$IWV = ZWD \cdot \frac{10^6}{R_w \left[k_2' + \frac{k_3}{Tm} \right]}. \quad (2)$$

In which, ZWD is multiplied by the specific constant for moist gases (R_w) and the refractivity constants (k_2' and k_3), along with the mean temperature (Tm), resulting in the IWV expressed in kg/m² (Sapucci, 2005).

The Tm can be accurately obtained from RDS data (Sapucci, 2001; Gouveia et al., 2020), by integrating the water vapour pressure (e, in hPa) and temperature (T, in Kelvin) as a function of altitude, expressed in Equation (3):

$$Tm = \frac{\int \frac{e}{T} dh}{\int \frac{e}{T^2} dh}. \quad (3)$$

The Tm can also be estimated using simplified models based on surface parameters, as will be presented in Section 2.3 for the computation of PWV-GNSS. Finally, the transformation from IWV to PWV is performed by applying the conversion factor for the density of liquid water (ρ_a), which is equivalent to 1 g/cm³ (Sapucci, 2001; Gouveia et al., 2020), as follow in Equation (4):

$$PWV = \frac{IWV}{\rho_a}. \quad (4)$$

Thus, by dividing the IWV by ρ_a, the PWV is obtained and expressed in millimetres. This value can be used for monitoring atmospheric water vapour.

2.4 PWV-GNSS from ZTD-SIRGAS

The PWV-GNSS can be obtained from the ZTD-SIRGAS by subtracting the ZHD from the ZTD, resulting in the ZWD. The ZHD is calculated using the Equation (5) proposed by Saastamoinen (1972), later refined by Davis et al. (1985):

$$ZHD = 0{,}0022779 \frac{P_s}{(1 - 0{,}0026 \cos 2\,\varphi - 0{,}00028h)}. \quad (5)$$

In which, the surface pressure (P_s) is expressed in hPa, while the latitude (φ) is given in radians and the station altitude (h) in metres. The input values for φ and h are obtained from the GNSS station (SMAR). Meanwhile, the surface atmospheric pressure used in the computation is measured at the INMET meteorological station (A803).

Considering that atmospheric pressure is correlated with altitude, it is important to note, as shown in Table 1, that the INMET station (A803) is located approximately 10 metres below the GNSS station (SMAR). Therefore, to adjust the surface pressure P_s measured at A803 to the altitude of the SMAR station, the Equation (6) described by (Berg, 1948) was applied:

$$P_{GNSS} \cong P_{MET}(1 - 0{,}0000226\,(h_{GNSS} - h_{MET}))^{5{,}225}, \quad (6)$$

where P_{MET} represents the atmospheric pressure measured at the INMET station (A803), and h_{GNSS} and h_{MET} are the altitudes of the GNSS and INMET stations, respectively. This procedure allows for the approximation of the surface pressure P_s measured at h_{MET} to the GNSS station altitude h_{GNSS}. By computing the ZHD using Equation (5) and applying the pressure adjustment from Equation (6), the GNSS-derived ZWD_{GNSS} can be obtained by a simple subtraction from the SIRGAS-derived ZTD_{SIRGAS}, as shown below in Equation (7):

$$ZWD_{GNSS} = ZTD_{SIRGAS} - ZHD. \quad (7)$$

Following the procedure to compute the PWV using Equation (2) and (4), it is necessary to use Tm . However, in this case, vertical profiles of temperature and water vapour are not available, since INMET automatic weather stations only provide surface-level parameters.

To address this limitation, an empirical model that estimates Tm based on surface temperature and pressure at the station altitude is applied. This approach, referred to as the "Brazilian model" is described by (Sapucci, 2005) as follows in Equation (8):

$$Tm = 0{,}558T_0 + 0{,}0105P_0 + 110{,}578, \quad (8)$$

where T_0 (K) and P_0 (hPa) represent the surface temperature and pressure, obtained from the INMET station A803. As previously performed for atmospheric pressure, a temperature adjustment procedure is applied to align the temperature value with the GNSS station elevation.

In order to accomplish this, the atmospheric lapse rate Equation (9) presented by National Geophysical Data Center (1992) was used, where T_{MET} is the surface temperature measured by the A803 station (in Kelvin), and T_{GNSS} is the temperature adjusted to the elevation of the GNSS station (h_{GNSS}).

$$T_{GNSS} \cong T_{MET} - (h_{GNSS}\ 0{,}0065). \quad (9)$$

Based on the estimated ZWD_{GNSS} and Tm calculated using Equation (8), Equations (2) and (4) were applied to convert the ZWD into IWV. Subsequently, the IWV values were converted into PWV-GNSS with an hourly sampling interval. These PWV-GNSS values were then used to analyse atmospheric water vapour variations during precipitation events.

2.5 Statistical Evaluation of PWV-GNSS against PWV-RDS

The validation of PWV-GNSS was carried out using data from the full year of 2023, with PWV-RDS serving as the reference. PWV-RDS measurements at 00 and 12 UTC were compared with corresponding PWV-GNSS values at the same times. To assess the quality of PWV-GNSS we calculated statistical metrics such as RMSE, bias, and R^2 using Equations (10), (11), and (12) from Willmott (1985).

$$RMSE = \sqrt{\frac{1}{n}\sum_{i=1}^{n}(P_i - O_i)^2}, \quad (10)$$

$$BIAS = \frac{1}{n}\sum_{i=1}^{n}(P_i - O_i), \quad (11)$$

$$R^2 = 1 - \frac{\sum_{i=1}^{n}(O_i - P_i)^2}{\sum_{i=1}^{n}(O_i - \bar{O})^2}, \quad (12)$$

where each metric is calculated based on the differences between the reference values (O_i) and the values to be evaluated, which are predicted or estimated (P_i).

3. Results

3.1 Validation of PWV-GNSS using PWV-RDS

The validation of PWV-GNSS was performed through a correlation analysis, as shown in Figure 3, which presents the scatter plot of PWV-GNSS versus PWV-RDS, along with the statistical metrics (RMSE, bias, and R^2) computed from the dataset. The scatter plot shows that the maximum discrepancy, close to 7 mm, occurred for PWV values between 40 and 50 mm when comparing PWV-GNSS and PWV-RDS. The analysis of PWV-GNSS compared to PWV-RDS in the 2023 data shows a strong correlation (R = 0.97) between the two measurements. The PWV-GNSS estimates have an RMSE of 2.37 mm compared to PWV-RDS.

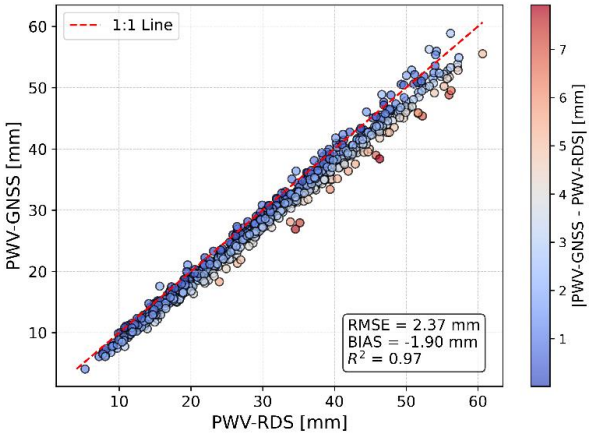

Figure 3. Statistical analysis of PWV-GNSS and PWV-RDS data for 2023 at 00 and 12 UTC, shown as a scatter plot with absolute differences represented by a colour bar, including RMSE, bias, and R^2 metrics.

The bias analysis shows that PWV-GNSS slightly underestimates PWV-RDS by 1.90 mm, accounting for about 80% of the RMSE. These results show that PWV-GNSS from ZTD-SIRGAS can reliably track atmospheric water vapour and help analyse rainfall events in the study area during September 2023.

3.2 Application of PWV-GNSS during precipitation events

Figure 4 presents the case study for September 2023 in Santa Maria (RS). The left axis shows the PWV values, with the black line representing PWV-GNSS and the red triangles showing PWV-RDS measurements. The blue lines depict hourly accumulated precipitation.

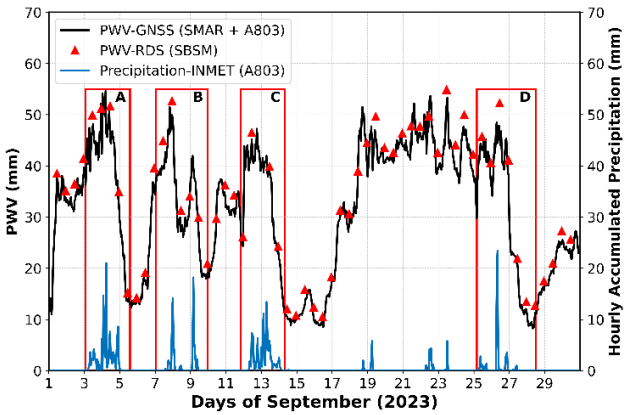

Figure 4. Comparison of PWV-GNSS (SMAR + A803) and PWV-RDS (SBSM) with Hourly Accumulated Precipitation (A803) for September 2023 in Santa Maria, RS.

Events A, B, C, and D illustrate jumps in PWV values preceding precipitation events (Sapucci, 2019), followed by further declines after rainfall. In event A, the PWV decreased by about 42 mm after accumulated precipitation totalling approximately 141 mm (from days 3 to 5). During event B (days 7 to 10), the PWV returned to around 50 mm but subsequently dropped to 18 mm following precipitation. During event B (days 7 to 10), the PWV returned to around 50 mm but subsequently dropped to 18 mm

following precipitation. This pattern was similarly observed in event C. Finally, event D recorded the highest hourly accumulated precipitation (23 mm), followed by the lowest PWV value observed (8 mm). However, the direct correlation between PWV and precipitation is not straightforward, since high PWV values do not always result in immediate rainfall. This is partly due to the low frequency of hourly precipitation events compared to the persistence of elevated atmospheric moisture levels, which statistically reduces the correlation between these variables.

PWV exhibited jumps above 50 mm at various times and responded to rainfall occurrences with sharp declines, reaching as low as 8 mm after precipitation. This analysis demonstrates that the PWV-GNSS methodology correlates well with precipitation events, confirming its effectiveness for monitoring atmospheric water vapour.

4. Conclusion

This work presents an alternative method for estimating PWV-GNSS by converting ZTD-SIRGAS data, first by removing the ZHD component and then computing PWV using the remaining ZWD and appropriate conversion factors. The methodology integrates a simplified and improved ZHD model, based on the approaches proposed by Saastamoinen (1972) and Davis et al. (1985), and employs techniques from Sapucci (2005) to estimate Tm, combined with automatic meteorological data from INMET. The method was validated against PWV-RDS, demonstrating high accuracy, with an RMSE of 2.37 mm, a bias of -1.90 mm (indicating a slight underestimation relative to PWV-RDS), and an R^2 of 0.97. Subsequently, the approach was applied in a case study conducted in September 2023 in Santa Maria (RS), a month that recorded 454 mm of accumulated rainfall, approximately 300 mm above the historical average, according to INMET.

The analysis of PWV derived from GNSS and RDS alongside hourly precipitation data showed that PWV responds dynamically to rainfall events. PWV-GNSS detected significant drops in atmospheric water vapour, up to 40 mm, following precipitation in cases A through D (Figure 4). Subsequently, PWV increased again, often preceding new rainfall, as observed between days 17 and 21.

Santa Maria (RS) is characterised by climatic instability and intense rainfall, highlighting the relevance of climatic studies and the integration of meteorological tools. PWV demonstrated the capability to capture abrupt atmospheric variations, with maxima reaching 50 mm and minima as low as 8 mm.

This study demonstrates a robust methodology to obtain PWV-GNSS based on GNSS and INMET meteorological stations, enabling precipitation event analysis and atmospheric water vapour monitoring via GNSS systems. The methodology offers a potential increase in temporal resolution compared to PWV-RDS by integrating both data sources. Based on these results, PWV-GNSS can be applicable for atmospheric monitoring and can be implemented in the analysis of extreme precipitation events and highly variable scenarios.

Future studies could explore the spatial coverage of the model and evaluate whether similar accuracy can be achieved using more distant meteorological stations. Although this study focuses on the applied evaluation of GNSS-derived PWV in Brazil, its results provide a solid basis for improving rainfall prediction models and developing new PWV estimation methods.
Future research will also assess ZTD from real-time Precise Point Positioning (PPP) to derive near real-time PWV-GNSS, and investigate techniques to detect PWV jump events (Sapucci, 2019) as indicators of imminent precipitation. Expanding analyses to other models, regions, and precipitation events will further strengthen the findings.

Acknowledgements

This study was financed in part by the National Council for Scientific and Technological Development, CNPq (grant n. 306112/2023-0, 33004129 and Finance Code 001, Grant Number 88887.817766/2023-00) and by the São Paulo Research Foundation, FAPESP (Grant: 2023/14739-0).

References

Albuquerque, A.M., Alves, D.B.M., Gouveia, T.A.F., Santos, V.A., 2022. Avaliação do atraso zenital hidrostático integrado e simplificado a partir de dados de radiossonda no território brasileiro. Presented at the XII Colóquio Brasileiro de Ciências Geodésicas e V Simpósio Brasileiro de Geomática, Curitiba - PR.

Albuquerque, A.M., Alves, D.B.M., Gouveia, T.A.F., Santos, V.A.D., Pompei, M.J.D.S., 2024. Análise do atraso úmido e hidrostático da atmosfera neutra por radiossondagem: estudo de caso para São Paulo (SP) e Manaus (AM) em períodos distintos. https://doi.org/10.5281/ZENODO.14116078

Albuquerque, A.M., Nespolo, R.S., Tommaselli, A.M.G., Martins-Neto, R.P., Imai, N.N., Alves, D.B.M., Gouveia, T.A.F., Jerez, G.O., 2024. Machine learning-based modelling of zenith wet delay using terrestrial meteorological data in the Brazilian territory. ISPRS Ann. Photogramm. Remote Sens. Spatial Inf. Sci. X-3–2024, 13–19. https://doi.org/10.5194/isprs-annals-X-3-2024-13-2024

Barry, R.G., Blanken, P.D., 2016. Microclimate and Local Climate. Cambridge, UK: Cambridge University Press.
Berg, H., 1948. Allgemeine meteorologie.

Bevis, M., Businger, S., Herring, T.A., Rocken, C., Anthes, R.A., Ware, R.H., 1992. GPS meteorology: Remote sensing of atmospheric water vapour using the global positioning system. J. Geophys. Res. 97, 15787–15801. https://doi.org/10.1029/92JD01517

Chapman, S., 1950. Upper atmospheric nomenclature. J. Geophys. Res. 55, 395–399. https://doi.org/10.1029/JZ055i004p00395

Davis, J.L., Herring, T.A., Shapiro, I.I., Rogers, A.E.E., Elgered, G., 1985. Geodesy by radio interferometry: Effects of atmospheric modeling errors on estimates of baseline length. Radio Science 20, 1593–1607. https://doi.org/10.1029/RS020i006p01593

De Lima, T.M.A., Santos, M., Alves, D.B.M., Nikolaidou, T., Gouveia, T.A.F., 2022. Assessing ZWD models in delay and height domains using data from stations in different climate regions. Appl Geomat 14, 93–103. https://doi.org/10.1007/s12518-021-00414-y

Elgered, G., Wickert, J., 2017. Monitoring of the Neutral Atmosphere, in: Teunissen, P.J.G., Montenbruck, O. (Eds.), Springer Handbook of Global Navigation Satellite Systems. Springer International Publishing, Cham, pp. 1109–1138. https://doi.org/10.1007/978-3-319-42928-1_38

Gong, Y., Liu, Z., Chan, P.W., Hon, K.K., 2023. Assimilating GNSS PWV and radiosonde meteorological profiles to improve the PWV and rainfall forecasting performance from the Weather Research and Forecasting (WRF) model over the South China. Atmospheric Research 286, 106677. https://doi.org/10.1016/j.atmosres.2023.106677

Gouveia, T.A.F., Monico, J.F.G., Alves, D.B.M., Sapucci, L.F., Geremia-Nievinski, F., 2020. 50 anos de sinergia entre Geodésia Espacial e Meteorologia: do erro no posicionamento GNSS a aplicações de previsão de precipitação de curtíssimo prazo. Rev. Bras. Cartogr. 72, 1509–1535. https://doi.org/10.14393/rbcv72nespecial50anos-56767

Hofmann-Wellenhof, B., Lichtenegger, H., Collins, J., 2001. Global Positioning System: theory and practice, 5th, rev. ed ed. Springer-Verlag, Wien.

Hopfield, H.S., 1971. Tropospheric Effect on Electromagnetically Measured Range: Prediction from Surface Weather Data. Radio Science 6, 357–367. https://doi.org/10.1029/RS006i003p00357

INMET, 2025. Nacional Institute of Meteorology. URL https://portal.inmet.gov.br/ (accessed 3.20.25).

Li, Q., Böhm, J., Yuan, L., et al., 2024. Global zenith wet delay modeling with surface meteorological data and machine learning. GPS Solut., 28, 57. https://doi.org/10.1007/s10291-023-01595-2

Liu, Y., Zhao, Q., Li, Z., Yao, Y., Li, X., 2022. GNSS-derived PWV and meteorological data for short-term rainfall forecast based on support vector machine. *Advances in Space Research* 70, 992–1003. https://doi.org/10.1016/j.asr.2022.05.057

Lu, C., Li, X., Zus, F., Heinkelmann, R., Dick, G., Ge, M., Wickert, J., Schuh, H., 2017. Improving BeiDou real-time precise point positioning with numerical weather models. J Geod 91, 1019–1029. https://doi.org/10.1007/s00190-017-1005-2

Montenbruck, O., Teunissen, P.J.G. (Eds.), 2017. Springer Handbook of Global Navigation Satellite Systems, 1st ed, Springer Handbooks. Springer, Cham. https://doi.org/10.1007/978-3-319-42928-1

National Geophysical Data Center, 1992. U.S. standard atmosphere (1976). Planetary and Space Science 40, 553–554. https://doi.org/10.1016/0032-0633(92)90203-Z

Nievinski, F.G., Santos, M.C., 2010. Ray-Tracing options to Mitigate the Neutral Atmosphere Delay in GPS. Geomatica 64, 191–207. https://doi.org/10.5623/geomat-2010-0020

RBMC, 2025. Brazilian Network for Continuous Monitoring of the GNSS Systems. URL https://www.ibge.gov.br/en/geosciences/geodetic-positioning/geodetic-networks/19213-brazilian-network-for-continuous-monitoring-of-the-gnss-systems.html (accessed 3.20.25).

Rohm, W., Yuan, Y., Biadeglgne, B., Zhang, K., Marshall, J.L., 2014. Ground-based GNSS ZTD/IWV estimation system for numerical weather prediction in challenging weather conditions. Atmospheric Research 138, 414–426. https://doi.org/10.1016/j.atmosres.2013.11.026

Rüeger, J.M., 2002. Refractive index formula for radio waves. In: Proc. XXII FIG Int. Congr., Washington, DC, USA, 19–26 Apr. Available: http://www.fig.net/resources/proceedings/fig_proceedings/fig_2002/Js28/JS28_rueger.pdf

SAPUCCI, L. F, 2005. Estimativas do IWV utilizando receptores GPS em bases terrestres no Brasil: sinergia entre a geodésia e a meteorologia (Doutorado em Ciências Cartográfica). Universidade Estadual Paulista (UNESP), Presidente Prudente – SP.

SAPUCCI, L. F, 2001. Estimativa do vapour d'água atmosférico e avaliação da modelagem do atraso zenital troposférico utilizando GPS (Mestrado em Ciências Cartográfica). Universidade Estadual Paulista (UNESP), Presidente Prudente – SP.

SAPUCCI, L.F., Machado, L.A.T., De Souza, E.M., Campos, T.B., 2019. Global Positioning System precipitable water vapour (GPS-PWV) jumps before intense rain events: A potential application to nowcasting. Meteorological Applications 26, 49–63. https://doi.org/10.1002/met.1735

Seeber, G., 2003. Satellite Geodesy. Walter de Gruyter. https://doi.org/10.1515/9783110200089

SIRGAS, 2025. Geocentric Reference System for the Americas. Tropospheric delays. URL https://www.sirgas.org/en/tropo-delays/ (accessed 3.20.25).

Thayer, G.D., 1974. An improved equation for the radio refractive index of air. Radio Science 9, 803–807. https://doi.org/10.1029/RS009i010p00803

UW, 2025. University of Wyoming. Atmospheric Science Radiosonde Archive. URL http://www.weather.uwyo.edu/upperair/sounding.shtml (accessed 3.20.25).

Valencia, M.A.C., Cruz, F.R.G., Balakit, R.B., 2019. LoRa Transmission System for Weather Balloons, in: Proc. IEEE 11th Int. Conf. Humanoid, Nanotechnol., Inf. Technol., Commun. Control, Environ. Manag. (HNICEM), Laoag, Philippines, pp. 1–5. https://doi.org/10.1109/HNICEM48295.2019.9072712

Vianello, R.L., Alves, A.R., 2012. Meteorologia básica e aplicações 2 ed. Editora UFV.

Wallace, J.M., Hobbs, P.V., 2006. Atmospheric science: an introductory survey, 2nd ed. ed, International geophysics series. Elsevier Academic Press, Amsterdam ; Boston.

Willmott, C.J., Ackleson, S.G., Davis, R.E., Feddema, J.J., Klink, K.M., Legates, D.R., O'Donnell, J., Rowe, C.M., 1985. Statistics for the evaluation and comparison of models. J. Geophys. Res. 90, 8995–9005. https://doi.org/10.1029/JC090iC05p08995

Xu, Z., Liu, W., Yan, W., Wang, X., Niu, Z., 2025. High-resolution PWV characteristics and response to precipitation in Northwest China based on GNSS. Theor Appl Climatol 156, 46. https://doi.org/10.1007/s00704-024-05265-2